

Pressure Effects on the Lamination of Organic Light-Emitting Diodes

Jing Du, Tiffany Tong, Wali Akande, Androniki Tsakiridou, and Wole Soboyejo

Abstract—This paper presents the results of finite element simulations of the lamination process for the fabrication of organic light-emitting diodes (OLEDs). The simulations utilize mechanical properties of the individual layers of the OLED structures that are obtained using nanoindentation techniques. The simulations show that applied pressure can cause contact evolution and sink-in around dust particles that are interposed between the organic materials layers, or the organic/inorganic layers. The implications of the results are discussed for the fabrication of robust OLEDs.

Index Terms—Finite element methods, light-emitting diodes (LEDs), materials testing, Young's modulus.

I. INTRODUCTION

ORGANIC light-emitting diodes (OLEDs) are layered structures that consist of successive organic layers that are stacked between a metallic cathode and an inorganic anode (Fig. 1) [1]. The diode itself is usually built on a transparent substrate (such as glass) that eventually forms the display through which the emitted light is observed. On top of this substrate, is a layer of indium tin oxide (ITO), that forms the anode of the diode. ITO is commonly used because it is highly conductive and transparent, thus allowing sufficient light to be transmitted from the diode. On top of the ITO anode, is a thin layer of poly(3, 4-ethylene dioxythiophene) (PEDOT) that is doped with poly(styrene sulphonate) (PEDOT:PSS).

Manuscript received March 06, 2012; accepted February 14, 2013. Date of publication April 05, 2013; date of current version August 07, 2013. This work was supported in part by the Division of Materials Research of the National Science Foundation through the MRSEC program at the Princeton Center for Complex Materials under Grant DMR-0819860, and in part by the Grand Challenges Program at Princeton University, Princeton, NJ, USA.

J. Du is with the Department of Mechanical and Aerospace Engineering and Princeton Institute for the Science and Technology of Materials (PRISM), Princeton University, Princeton, NJ 08544 USA (e-mail: jingdu@alumni.princeton.edu).

T. Tong is with the Department of Electrical Engineering and Princeton Institute for the Science and Technology of Materials (PRISM), Princeton University, Princeton, NJ 08544 USA, and the Center for Technology and Economic Development, New York University at Abu Dhabi, United Arab Emirates (e-mail: ttong@nyu.edu)

W. Akande is with the Department of Electrical Engineering and Princeton Institute for the Science and Technology of Materials (PRISM), Princeton University, Princeton, NJ 08544 USA (e-mail: wali.akande@gmail.com).

A. Tsakiridou is with the Picker Engineering Program, Smith College, Northampton, MA 01063 USA (e-mail: atsakiri@smith.edu).

W. Soboyejo is with the Department of Mechanical and Aerospace Engineering and Princeton Institute for the Science and Technology of Materials (PRISM), Princeton University, Princeton, NJ 08544 USA, and the African University of Science and Technology (AUST), Abuja, Federal Capital Territory, Nigeria (e-mail: soboyejo@princeton.edu)

Color versions of one or more of the figures are available online at <http://ieeexplore.ieee.org>.

Digital Object Identifier 10.1109/JDT.2013.2253085

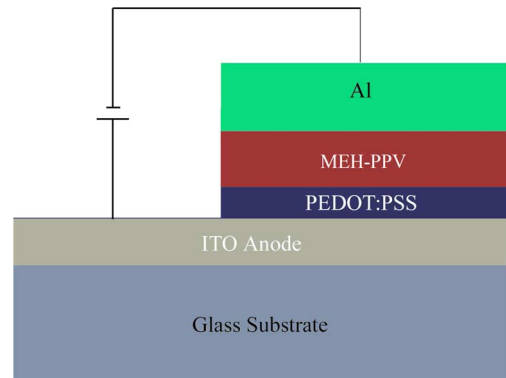


Fig. 1. Schematic of a typical OLED structure.

This is used to facilitate hole injection from the anode into the active layer. Next, the photo-emissive active layer of the OLED is deposited. This is the layer in which electrons and holes supplied by the cathode and anode recombine to generate light. One material used to form the active layer is poly[2-methoxy-5-(2'-ethyl-hexyloxy)-1,4-phenylene vinylene] (MEH:PPV), with molecular weight between 150,000 and 250,000. This produces a reddish-orange light with a peak emission around 550 nm. To complete the diodes, conventional shadow masks were used to pattern ~ 50 nm of aluminum to form the cathode layer.

Lamination [1], [2] and cold welding [3] are both low cost OLED fabrication processes. Cold welding is used to join metallic materials, while lamination usually involves polymeric materials. In both processes, the material that is being transferred is first deposited onto a patterned stamp. This is then pressed onto the substrate at a prescribed pressure and temperature. The material that is being transferred from the stamp to the substrate is left behind on the substrate when the stamp is lifted. In the cold welding process, Kim and Forrest [3], [4] found that the pressures required to fabricate OLEDs could be 1000 times different when using flexible polydimethyl-siloxane (PDMS) or rigid Si stamps. Cao *et al.* [5] later used the finite element simulations to analyze the effects of dust particles and layer properties on the fabrication of OLEDs. Lee *et al.* [1] and Rhee *et al.* [2] both demonstrated the transfer of metallic cathode by the lamination method. Kim *et al.* also [6] observed the OLEDs fabricated under pressure exhibited a notable increase in luminance intensity and current efficiency, when compared with pressure-free diodes.

In this work, nanoindentation techniques were used to characterize the mechanical properties of PEDOT:PSS and MEH-PPV that are relevant to OLED structures. These properties, along with published data for the other materials that were used in the

model OLED structure (Fig. 1) that was analyzed, were incorporated into finite element models that were used for the simulation of the lamination process. The models explored the effects of applied pressure on the laminated structures with dust particles interspersed between the stamp and substrate surfaces. The results show that pressure effects on the electrical properties of OLEDs can be explained by the increase of contact area. This paper also examines the effects of substrate modulus on the contact area and deformation around dust particles. The implications of the current results are then discussed for the fabrication of robust organic electronic diodes.

II. EXPERIMENTS

Baytron P VP Al-4083 PEDOT:PSS (now Heraeus Clevis, Hanau, Germany) was used as the hole injection layer in this study. It was chosen because of its reduced mean particle size and narrower size distribution. This reduces electrical “shorts” in the diode and smoothens the surface. It was filtered through a 0.2 μm filter to further improve the smoothness and uniformity. This was done for 1 minute at a rate of 3000 revolutions per minute (rpm). The filtered solution was then spin-coated onto a glass substrate at 250 rpm for 15 s. This was used to attain thicknesses of around 750 nm, as measured using a KLA-Tencor P15 Surface Profiler (KLA-Tencor, Milpitas, CA). The samples were then cured at 120 °C for 5 minutes to remove any residual moisture.

The MEH-PPV (Sigma Aldrich, St. Louis, MO) was mixed with chloroform at a 5 g/L ratio. The mixture was then covered and stirred continuously for at least 6 hours at room temperature. The mixture was passed through a 0.45 μm Teflon¹ filter. The filtered solution was then spin-coated onto a glass substrate at 500 rpm for 15 s. This was used to attain MEH-PPV layer thicknesses of around 120 nm, as measured using the same surface profiler described earlier.

Nanoindentation measurements were carried out on the PEDOT:PSS and MEH-PPV thin films, respectively. The experiments were performed with a TriboScope nanomechanical testing system (Hysitron Inc., Minneapolis, MN), coupled to a Dimension 3100 scanning probe microscope (Veeco Instruments Inc., Woodbury, NY). A Berkovich indenter tip, a three sided pyramidal-type tip with an included angle of 142.3°, was used. This was chosen for its large angle, hence large contact area, with the samples. The loading profile consisted of the following three steps: loading to a peak load, holding at the peak load, and returning to zero load. For PEDOT:PSS, a peak load of 200 μN , a loading rate of 40 $\mu\text{N/s}$, a holding period of 6 minutes, and a unloading rate of 40 $\mu\text{N/s}$ were applied. In the case of MEH-PPV, a peak load of 50 μN , a loading rate of 10 $\mu\text{N/s}$, a holding period equal to or longer than 2 minutes, and an unloading rate of 10 $\mu\text{N/s}$ were applied.

To minimize the possible interactions between adjacent indents, all the indents were separated by 10 μm . Commonly, for metallic materials, indentation depths should be at least 20 times greater than the average surface roughness to minimize the possible effects of rough surfaces [7]. Although, indentation depths

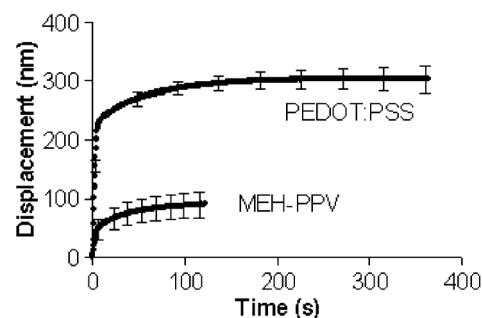


Fig. 2. Creep behavior of PEDOT:PSS and MEH-PPV under constant loading.

TABLE I
MEASURED YOUNG'S MODULUS AND COMPARISON WITH LITERATURES

Polymer	Young's Modulus (GPa)	Method	Reference
PEDOT:PSS	1.42±0.07	nanoindentation	Current Study
	0.9~1.9	dog-bone tensile test	Ref. [9]
	2.26±0.05	buckling	Ref. [10]
MEH-PPV	11.5±2.2	nanoindentation	Current Study
	11.7±2.0	nanoindentation	Ref. [11]

less than 10% of the film thickness minimize the substrate effects [8]. While using this rule is experimentally feasible for thick films that are greater than a micrometer in thickness, this approach could be hard to apply on very thin polymer films.

To minimize the influence of viscoelasticity and to ensure that only the instantaneous responses of the polymers films were measured, a sufficiently rapid unloading rate (40 $\mu\text{N/s}$ for PEDOT:PSS and 10 $\mu\text{N/s}$ for MEH-PPV) and a long holding period (6 minutes for MEH-PPV and 2 minutes for PEDOT:PSS) were applied. Fig. 2 shows the viscoelastic creep of PEDOT:PSS and MEH-PPV. These correspond to the average of 5 samples. As shown in Fig. 2, the two polymers are both fully relaxed during the holding period.

The measured Young's moduli were compared with prior measurements in Table I. Lang *et al.* [9] measured the Young's modulus of PEDOT:PSS to be in the range between 1.9 and 0.9 GPa at a relative humidity between 40% and 55%. This is in agreement with the Young's modulus of 1.56 ± 0.08 GPa measured in the nanoindentation in this study at a relative humidity of 42%. Tahk *et al.* measured the Young's modulus of PEDOT:PSS to be 2.26 ± 0.05 GPa [10]. This is slightly higher than the value reported by Lang *et al.* [9] and those obtained in this study. The higher values reported by Tahk [10] are attributed to potential effects of plasticity on the buckled profiles that were used to estimate the Young's moduli. The Young's modulus of MEH:PPV was measured by McCumiskey (using the nanoindentation method) to be ~ 11.7 ± 2.0 GPa [11]. This is in close agreement with the Young's modulus of 11.5 ± 2.2 GPa that was obtained from the current work using nanoindentation.

III. FINITE ELEMENT MODELING

It has been shown by Moreau *et al.* [12], [13] that dust particles in the clean room environment include silicon, iron, aluminum, quartz, textile polymer, silicone and photoresist. The

¹Teflon is a trademark of DuPont.

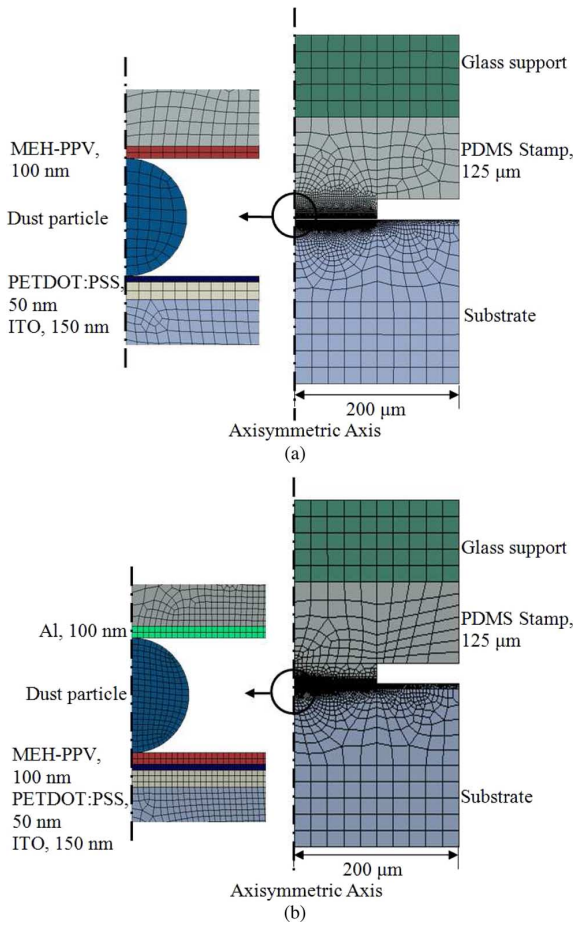


Fig. 3. Finite element model geometry and mesh. (a) Finite element model for lamination of MEH-PPV on PEDOT:PSS. (b) Finite element model for lamination of aluminum on MEH-PPV.

typical dust particle diameter ranges from ~ 0.1 – $20 \mu\text{m}$. In the lamination processes, the dust particles interposed between the stamp and the substrate. They therefore affect the evolution of the contact areas. Cao *et al.* [5] have shown that, in the cold welding processes, soft stamps are expected to deform easily around such dust particles at relatively low pressures. However, considerably higher pressures are needed to deform stiff stamps over similar contact areas.

This paper examines the effects of pressures on the lamination on layers that are relevant to OLEDs. Finite element simulations of the lamination processes were conducted using the Abaqus software package (Dassault Systèmes Simulia Corporation, Providence, RI). These include the lamination of MEH-PPV to PEDOT:PSS and the lamination of aluminum to MEH-PPV. The effects of dust particles were considered in the simulations of contact between polymer (MEH-PPV) and polymer (PEDOT:PSS) and metal (aluminum) and polymer (MEH-PPV).

The simulation considered a pattern of the diode in an array of $200 \mu\text{m}$ diameter posts, with a $400 \mu\text{m}$ spacing, as described by Kim and Forrest [4]. Axisymmetric geometries were used to simplify the cylindrical geometry of the diodes. Two typical finite element models are shown in Fig. 3. Fig. 3(a) shows a MEH-PPV-coated stamp about to be laminated onto a PEDOT:PSS

TABLE II
MATERIAL PROPERTIES USED IN THE FINITE ELEMENT SIMULATIONS

Material	Young's modulus (GPa)	Poisson's Ratio	Reference
PDMS	0.003	0.48	Ref. [14], [15]
Al	70	0.3	Ref. [16]
PEDOT:PSS	1.42	0.3	Current Study
MEH-PPV	11.5	0.3	Current Study
ITO	116	0.35	Ref. [17]
Glass	69	0.3	Ref. [16]
PET	2.5	0.3	Ref. [18]
Particle	70	0.3	Ref. [5]

layer. Fig. 3(b) shows an aluminum-coated stamp about to be laminated onto a MEH-PPV layer. Note that the material and thickness of each layer are marked in the figure. The diameter of dust particle was chosen to be $1 \mu\text{m}$. A 4-node bilinear axisymmetric quadrilateral element was used in the mesh. The mesh was dense in the regions near the dust particle and the contact surfaces. Similar mesh sizes were also used in the regions near the surface contact regimes.

It was assumed that all the materials exhibited isotropic elastic behavior. Young's moduli were obtained from the nanoindentation experiments described earlier in this work as well as from prior studies [5], [14]–[18]. However, the results from the current study were also compared to Young's moduli obtained from other studies in which nanoindentation [11], micro-tensile [9] and micro-buckling [10] techniques were used (Table I). The Young's modulus and Poisson's ratio of each material used in the simulation were summarized in Table II.

The axisymmetric boundary condition was applied at the symmetry axis (Fig. 3). The bottom of the substrate was fixed to have no displacements and rotations. The outer edge of the model was fixed to have no lateral movement for continuity. The top of the stamp moved downward. The reaction forces at the top of the stamp were determined and used to simulate the pressure applied during the lamination process.

For simplicity and convergence, frictionless contact was assumed between the dust particle and the stamp, and also between the dust particle and the substrate. Considering the adhesion interaction between the substrate and the stamping material, rough contacts were used to ensure that there were no relative sliding, after the substrate and the stamping material were brought into contact.

IV. RESULTS AND DISCUSSION

A. Effects of Pressure

A typical calculated profile of an MEH-PPV-coated stamp on a PEDOT:PSS on PDMS substrate under pressure is presented in Fig. 4. The stamp has clearly deformed around the dust particle and made contact with the substrate. The ratio of the contact length, L_c , to the overall total length, L , can be used to characterize the efficiency of the lamination process. It is also important to note that Fig. 4 also shows that the stamp and the dust particle sank into the substrate, due to the applied pressure.

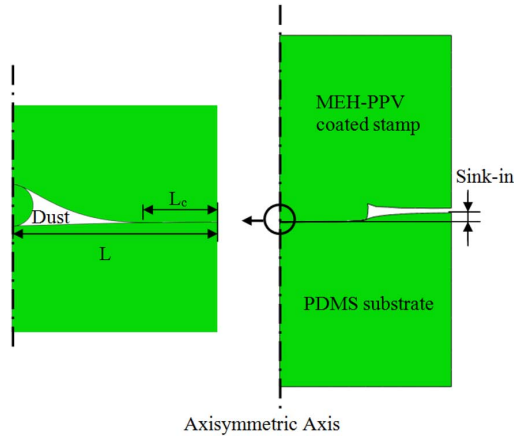


Fig. 4. Calculated deformed profile for lamination of MEH-PPV with PDMS substrate at a pressure of 100 kPa.

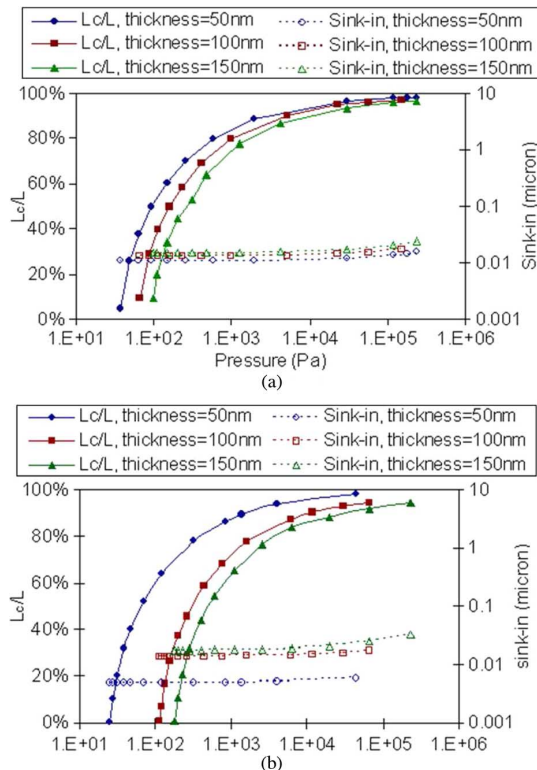


Fig. 5. Dependence of transferring material thickness in the lamination processes. (a) Contact length and sink-in depth vs pressure during the lamination of MEH-PPV. (b) Contact length and sink-in depth vs pressure during the lamination of aluminum.

Hence, the lowest point of the substrate surface was right beneath the dust particle, while the highest point of the substrate was on the right-hand side, close to the edge of the model. This corresponds to the mid-point between two posts.

The height difference between the highest and lowest points was defined as the sink-in depth. This was used to characterize the damage to the substrate. The contact lengths and the sink-in depths both increased with increasing pressure, as shown in Figs. 5 and 6. However, the rate of increase of the contact length decreased for contact length ratios above $\sim 80\%$. In contrast, the rate of increase of the sink-in depth was low for contact length

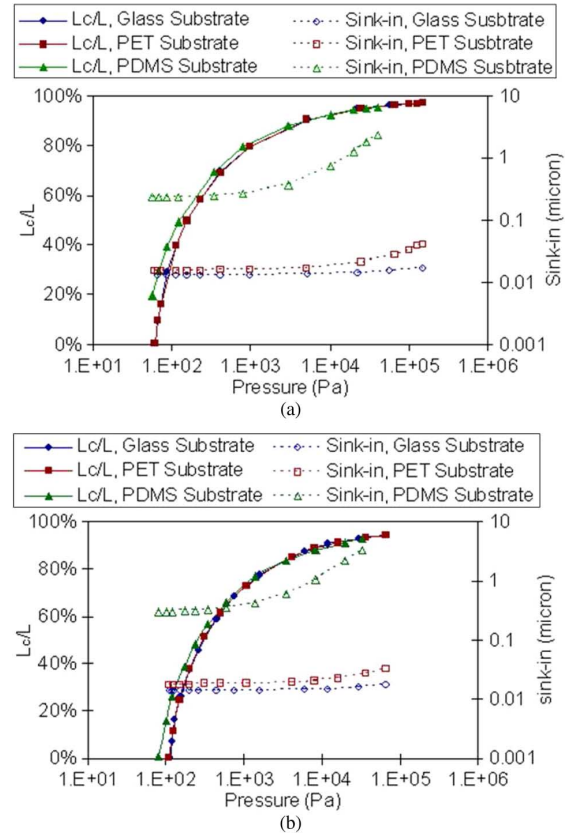


Fig. 6. Dependence of substrate material in the lamination processes. (a) Contact length and sink-in depth vs pressure during the lamination of MEH-PPV. (b) Contact length and sink-in depth vs pressure during the lamination of aluminum.

ratios below $\sim 80\%$. However, the rate of increase of sink-in depth increased at higher pressures, especially when the contact length ratios were greater than $\sim 80\%$ (Figs. 5 and 6). This phenomenon indicates that adequate amount of pressure could be helpful for the lamination efficiency, but the excess pressure might be harmful to the diode.

B. Effects of Layer Thickness

The advantages of soft stamps have been demonstrated in prior work [1], [4], [5]. These have shown that the contact lengths increase with decreasing stamp modulus. However, the effects of transfer layer thickness have received less attention [5]. The current work shows that lower pressures are needed to induce the same contact length ratios during the transfer of thinner polymer films [Fig. 5(a)]. The effects are even more evident during the transfer of stiffer materials, such as aluminum [Fig. 5(b)]. The results showed that when the pressure is ~ 200 Pa, a transfer layer thickness of 150 nm resulted in contact length ratio of $\sim 20\%$, while a transfer layer thickness of 50 nm resulted in a contact length ratio of $\sim 75\%$. These results suggest that the overall contacts depend largely on the overall stiffnesses of the stamping structures, i.e. the coated stamps.

The computed sink-in depths also increased with increasing transfer layer thickness [Fig. 5]. This was particularly evident in the results obtained for the lamination of aluminum [Fig. 5(b)]. The results showed that transfer layer thickness of

50 nm resulted in sink-in depths of $\sim 0.005\text{--}0.006\ \mu\text{m}$, while transfer layer thickness of 150 nm resulted in sink-in depth of $\sim 0.2\text{--}0.3\ \mu\text{m}$. Increasing transfer layer thickness also increased the sink-in depths during the transfer of MEH-PPV [Fig. 5(a)]. However, the effects of transfer layer thickness are less evident [Fig. 5(a)].

C. Effects of Substrate Modulus

It is important to examine the effects of substrate moduli that are relevant to rigid, flexible and stretchable organic electronic structures. The current work shows that stretchable PDMS structures with moduli of $\sim 0.003\ \text{GPa}$ resulted in the highest levels of sink-in [Fig. 6], while rigid glass substrate with moduli of 70 GPa are associated with the lowest levels of sink-in. PET substrates with intermediate moduli resulted in intermediate levels of sink-in [Fig. 6]. In contrast, substrate moduli did not have significant effects on contact length ratios above $\sim 80\%$. However, some effects were observed at lower contact length ratios, where the lower modulus PDMS substrate resulted in higher contact length ratios [Fig. 6].

D. Implications

In addition to understanding the effects of pressure, layer thickness and substrate materials, the results obtained from the current simulations provide insights that could guide the future optimization of the lamination process of flexible/stretchable/rigid organic electronic diodes. The current results show that the application of pressure promotes improved contact between the layers that are relevant to OLED structures (Fig. 5 and 6). The improved contact could facilitate the successful transfer of the laminating material. It could also improve the electronic properties of the laminated devices. However, excessive pressure could result in sink-in and damage to the devices. This might result in the defective pixels on the display.

Furthermore, consideration has to be given to the selection of layer thicknesses of transfer material in the design of organic electronic diodes. Thicker layers result in diode architectures that are more structurally stable, while thinner layer might result in improved contact and adhesion, hence better electronic properties. Also, in applications that require the use of flexible polymer substrates, special considerations should be given to the selection of the substrate materials. A softer substrate could be more flexible/stretchable, but could also be vulnerable to pressure.

V. CONCLUSION

This paper presents the results of a study of the lamination of OLEDs. Nanoindentation measurements of the Young's modulus and viscoelastic properties of PEDOT:PSS and MEH-PPV thin films were incorporated into finite element simulations of the lamination process. These were used to study the effects of pressure, layer thickness and the substrate Young's modulus. The results suggest that an appropriate pressure is needed to balance the lamination efficiency and the damage of the diode. Thinner transfer films were also shown to require lower pressures, while inducing less damage in the diode. However,

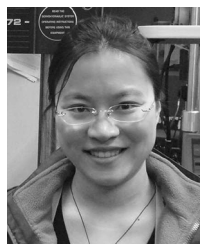
thinner films are less stable structurally. Hence, an optimized film thickness has to be found. Furthermore, soft substrates for flexible/stretchable organic electronic diodes need to be selected carefully to have stiffness within a range. Too soft a substrate could result in device damage during the lamination process, and inadequate stiffness to support the structure. Conversely, stiff substrate could limit the surface contacts in ways that could compromise the device.

ACKNOWLEDGMENT

The authors are grateful to Prof. L. Lei of Tsinghua University, and Dr. Y. Cao for useful technical discussions. Appreciation is also extended to Mr. J. Palmer for his technical assistance.

REFERENCES

- [1] T.-W. Lee, J. Zaumseil, Z. Bao, J. W. P. Hsu, and J. A. Rogers, "Organic light-emitting diodes formed by soft contact lamination," *Proc. Nat. Acad. Sci. USA*, vol. 101, no. 2, pp. 429–433, Jan. 2004.
- [2] J. Rhee and H. H. Lee, "Patterning organic light-emitting diodes by cathode transfer," *Appl. Phys. Lett.*, vol. 81, no. 22, p. 4165, 2002.
- [3] C. Kim, "Micropatterning of organic electronic devices by cold-welding," *Science*, vol. 288, no. 5467, pp. 831–833, May 2000.
- [4] C. Kim and S. Forrest, "Fabrication of organic light-emitting devices by low-pressure cold welding," *Adv. Mater.*, vol. 15, no. 6, pp. 541–545, 2003.
- [5] Y. Cao, C. Kim, S. R. Forrest, and W. Soboyejo, "Effects of dust particles and layer properties on organic electronic devices fabricated by stamping," *J. Appl. Phys.*, vol. 98, no. 3, pp. 033713–033713-6, 2005.
- [6] J. H. Kim, S.-M. Seo, and H. H. Lee, "Nanovoid nature and compression effects in organic light emitting diode," *Appl. Phys. Lett.*, vol. 90, no. 14, p. 143521, 2007.
- [7] *Metallic Materials, Instrumented Indentation Test for Hardness and Materials Parameters—Part 1: Test Method*, ISO 14577-1:2002, International Organization for Standardization, Geneva, Switzerland, 2002.
- [8] W. C. Oliver and G. M. Pharr, "An improved technique for determining hardness and elastic modulus using load and displacement sensing indentation experiments," *J. Mater. Res.*, vol. 7, no. 6, pp. 1564–1583, Jan. 2011.
- [9] U. Lang, N. Naujoks, and J. Dual, "Mechanical characterization of PEDOT:PSS thin films," *Synth. Metals*, vol. 159, no. 5–6, pp. 473–479, Mar. 2009.
- [10] D. Takh, H. H. Lee, and D.-Y. Khang, "Elastic moduli of organic electronic materials by the buckling method," *Macromolecules*, vol. 42, no. 18, pp. 7079–7083, Sep. 2009.
- [11] E. J. McCumiskey, N. Chandrasekhar, and C. R. Taylor, "Nanomechanics of CdSe quantum dot-polymer nanocomposite films," *Nanotechnology*, vol. 21, no. 22, p. 225703, May 2010.
- [12] W. M. Moreau, *Semiconductor Lithography: Principles, Practices, and Materials*. New York, NY, USA: Plenum, 1988.
- [13] *Cleanrooms Of, and Associated Controlled Environments—Part 1: Classification of Air Cleanliness*, ISO 14644-1:1999, International Organization for Standardization, Geneva, Switzerland, 1999.
- [14] A. Bietsch and B. Michel, "Conformal contact and pattern stability of stamps used for soft lithography," *J. Appl. Phys.*, vol. 88, no. 7, p. 4310, 2000.
- [15] N. Bowden, S. Brittain, A. G. Evans, J. W. Hutchinson, and G. M. Whitesides, "Spontaneous formation of ordered structures in thin films of metals supported on an elastomeric polymer," *Nature*, vol. 393, no. May, p. 146, 1998.
- [16] W. Soboyejo, *Mechanical Properties of Engineered Materials*. Boca Raton, FL, USA: CRC, 2003, vol. 152.
- [17] D. Neerincx and T. J. Vink, "Depth profiling of thin ITO films by grazing incidence X-ray diffraction," *Thin Solid Films*, vol. 278, no. 1–2, pp. 12–17, May 1996.
- [18] A. Aref-Azar, F. Biddlestone, J. N. Hay, and R. N. Haward, "The effect of physical ageing on the properties of poly(ethylene terephthalate)," *Polymer*, vol. 24, no. 10, pp. 1245–1251, Oct. 1983.



Jing Du received the B.S. and M.S. degrees from the Department of Mechanical Engineering at Tsinghua University, China, in 2005 and 2007, respectively, and is currently working toward the Ph.D. degree in the Department of Mechanical & Aerospace Engineering at Princeton University, Princeton, NJ, USA. Her research areas are materials science and solid mechanics.

Her research interests include organic electronic devices, biomedical devices, bio-inspired design, and nanomaterials.



Tiffany Tong received the B.S. degree in electrical engineering at the University of California, Los Angeles, CA, USA, and the M.A. and Ph. D. degrees from the Department of Electrical Engineering at Princeton University, Princeton, NJ, USA. Her doctoral research focused on the study of adhesion and interfacial fracture in organic light emitting devices and photovoltaic cells.

She is currently a research associate at the Center for Technology and Economic Development at New York University in Abu Dhabi, United Arab

Emirates.

Wali Akande, photograph and biography not available at time of publication.

Androniki Tsakiridou, photograph and biography not available at time of publication.



Wole Soboyejo was educated at King's College London, London, U.K., and the University of Cambridge, Cambridge, U.K..

In 1988, he joined The McDonnell Douglas Research Labs in St. Louis, MO, USA, as a research scientist. In 1992, he worked briefly as a Principal Research Engineer at the Edison Welding Institute before joining the Engineering Faculty of The Ohio State University, Columbus, OH, USA. From 1997 to 1998, he was a Visiting Professor in the Departments of Mechanical Engineering and Materials Science and engineering at MIT, Cambridge, USA. In 1999, he was appointed as a Professor of Mechanical and Aerospace Engineering at Princeton University, Princeton, NJ, USA. He is also the Director of the Undergraduate Program in Materials at the Princeton Institute of Science and Technology of Materials. His research focuses on experimental studies of biomaterials and the mechanical behavior of materials. His current areas of interest include micromechanical machines, nanoparticles for disease detection, biomedical systems for prostheses, and cardiovascular systems, infrastructure materials, and alternative energy systems.